ELSEVIER

Treatment of wastewater from synthetic textile industry by electrocoagulation–electrooxidation

G. Bhaskar Raju [a], M. Thalamadai Karuppiah [a,b,*],
S.S. Latha [a], S. Parvathy [a], S. Prabhakar [a]

[a] *National Metallurgical Laboratory Madras Centre, CSIR Madras Complex, Taramani, Chennai 600113, India*
[b] *Central Ground Water Board, Besant Nagar, Chennai 600090, India*

Abstract

Treatment of wastewater from a textile industry that produces synthetic polyester cloths was studied employing electrochemical techniques. The sample was initially subjected to electrocoagulation to remove suspended solids. Mild steel and aluminum electrodes were tried as anodes; and aluminum was found to be effective for the removal of suspended solids. Using aluminum as anode, the chemical oxygen demand (COD) concentration of the effluent which was initially at the level of $1316 \, \text{mg L}^{-1}$ could be reduced to $429 \, \text{mg L}^{-1}$ by electrocoagulation. After electrocoagulation, the effluent was further subjected to electrooxidation using graphite and $RuO_2/IrO_2/TaO_2$ coated titanium as anodes. During the electrooxidation tests, both COD and chloride ion were simultaneously estimated; and the effect of Cl^- ion is discussed. The measurements have revealed the depletion of Cl^- ion concentration implying the generation of free chlorine during electrooxidation. The depletion of Cl^- ion concentration and the COD removal were observed to be comparatively high in the presence of graphite electrode. The effects of electrode materials and current density on COD removal are discussed. The instantaneous current efficiency (ICE), mass transfer coefficient and energy consumption were estimated.
© 2008 Elsevier B.V. All rights reserved.

Keywords: Purification; Graphite electrode; $RuO_2/IrO_2/TaO_2$ coated Ti electrode; COD; Instantaneous current efficiency

1. Introduction

The textile dyeing and finishing industries generate large quantity of wastewater containing unreacted dyes, suspended solids, dissolved solids, and other auxiliary chemicals. Depending on the reactivity of the dyes, 10–20% of the dyes used remain dissolved in water. The wastewaters, containing especially azo dyes, are toxic and mutagenic to microbes and fish species. Hence, removal of dyes from the effluent has been gained greater attention of many researchers. Though the biological treatment is the most efficient and economically attractive process for the treatment of industrial effluents, this method is rarely employed for textile effluents because they are recalcitrant to biodegradation. The biodegradation is inhibited in the presence of toxic byproducts and toxic dye additives. Therefore,

advanced oxidation processes (AOP) that rely on the generation of very reactive short lived hydroxyl radicals has been attempted to decontaminate the textile wastewater. The efficiency of AOP in the presence of dyeing auxiliaries, such as NaCl, Na_2CO_3 and Na_2SO_4, as well as dyeing process oriented additives like sequestering agents, surfactants and anticreasing agents is poor. Most dyeing auxiliaries are known to scavenge hydroxyl radicals and hence expected to seriously inhibit the treatment efficiency of advanced oxidation processes. AOP have been successfully employed for color removal from aqueous reactive dye solutions, but found to be rather inefficient for ultimate oxidation to meet discharge standards and/or re-use of spent dye house effluent in the dyeing process [1–3]. The problems are becoming more complex with the usage of newer dyestuffs that are far more resistant to degradation.

In recent years, the electrochemical techniques have received greater attention, because all types of pollutants could be removed effectively. In electrooxidation, the main reagent is the electron (clean reagent) that 'incinerates' the organics without generating any secondary pollutants. Electrocoagulation was reported to be very effective for the decolorization of orange II

* Corresponding author at: National Metallurgical Laboratory Madras Centre, CSIR Madras Complex, Taramani, Chennai 600113, India.
Tel.: +91 44 22542077; fax: +91 44 22541027.
E-mail address: mtkaruppiah@gmail.com (M.T. Karuppiah).

dye [4] and purification of textile wastewater [5]. The combination of electrocoagulation using iron and electrooxidation using graphite electrodes was observed to be effective for the removal of CI Acid orange 10 [6]. Activated carbon fiber (ACF) and granulated graphite were tried as cathodes for the reduction of vat dyes [7,8]. Though the chromaticity of the dyes could be eliminated, the chemical oxygen demand (COD) removal was observed to be only partial. The electrochemical degradation of acid orange 7 and amaranth dyestuff was studied using boron doped diamond electrodes [9,10]. Though these electrodes were proved to be effective, their commercial viability is yet to be ascertained. The removal of COD to the extent of 80% from textile wastewater was reported using Pt/Ti electrode [11,12]. The effectiveness of Ti/RuO_2, Ti/Pt and Ti/Pt/Ir electrodes for the treatment of textile wastewater were studied and found that the COD of the effluent could be removed to the extent of 85%. The electrochemical oxidation of organic substances was attributed to OCl^-, OH^-, nascent oxygen and other reactive species generated *in situ* during electrolysis.

The continuous depletion of groundwater, shortage in rainfall and huge consumption of water by textile industries has necessitated the recycling and re-use of processed water. The State Pollution Control Board of Tamilnadu, India has directed the textile industries to implement zero discharge facilities within a defined timeframe. The other States in India are likely to follow suit in implementing the zero discharge concepts. Various technological options are being studied to recover the water for re-use. The combination of electrocoagulation/electroflotation, electrooxidation, filtration and reverse osmosis is being tried on a priority basis to address the environmental issues of textile effluents. In tune with such efforts, the effectiveness of electrochemical methods for the treatment of wastewater from a textile industry manufacturing 2400 tonnes per annum of synthetic polyester cloth was attempted in the present study. The effectiveness of two different anode materials namely graphite and $RuO_2/IrO_2/TaO_2$ coated titanium was studied.

2. Materials and methods

2.1. Electrochemical cell

An acrylic tank with a working volume of about 3 L, fitted with electrodes was used to conduct the experiments. Mild steel and aluminum rods, with a minimum purity of 98% and each rod measuring 0.6 cm diameter and 11 cm length were used as electrodes for electrocoagulation. Six such rods, connected to a common rod, formed the anode assembly and an equal number of rods with similar arrangement formed the cathode assembly. The gap between the anode and cathode was maintained at 2 mm to minimize the ohmic losses. The entire electrode assembly (undivided electrolytic cell) was placed on nonconducting wedges fixed to the bottom plate of the electrocoagulation tank. For electrooxidation, two different materials, viz.
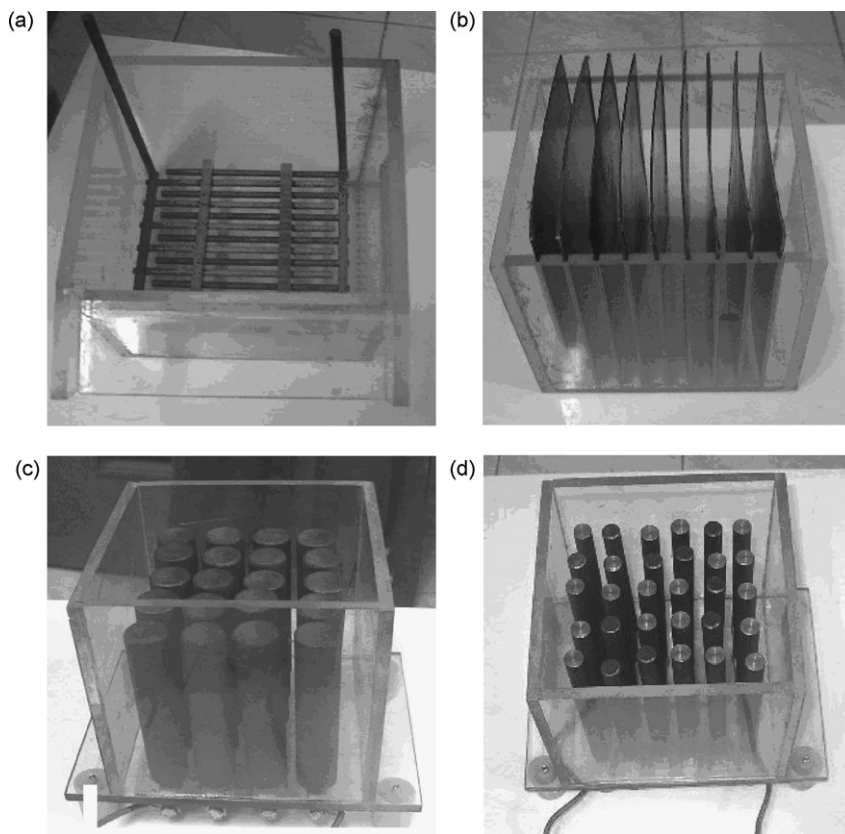

Fig. 1. Photographs showing arrangement of electrodes. (a) Electrocoagulation cell. (b) Electrooxidation cell with graphite sheets. (c) Electrooxidation cell with graphite rods. (d) Electrooxidation cell with $RuO_2/IrO_2/TaO_2$ coated titanium rods.

$RuO_2/IrO_2/TaO_2$ coated titanium rods and graphite in the form of sheets and also rods were used. A set of five graphite rods were connected to a common copper plate from the bottom of the tank. Four such set of electrodes (two for anode and two for cathode) were used. The alternate sets looped internally form anode and cathode assembly. Similar arrangement of electrodes (three for anode and three for cathode) was followed in the case of $RuO_2/IrO_2/TaO_2$ coated titanium electrodes. The gap between anodes and cathodes was maintained at 6 mm. The arrangement of the electrodes, both for electrocoagulation/flotation and electrooxidation, are shown in Fig. 1.

2.2. Effluent sample

The representative wastewater sample was collected over a period of 12 h from a textile industry that produces synthetic polyester fabric. The characteristics of the wastewater sample and the size distribution of suspended solids are shown in Table 1 and Fig. 2.

2.3. Electrode materials

The $RuO_2/IrO_2/TaO_2$ coated titanium rods with a coating thickness of 6 mm were obtained from M/s Titanium and Tantalum Products, India. The graphite materials used in the present study were obtained from M/s Carbone Lorraine. The electrical resistivity of graphite sheets was 0.001 Ω cm. The graphite sheet assays 99.8% C, <150 mg L^{-1} of Fe and <30 mg L^{-1} of Cl. The respective anodic surface area of graphite rods, graphite sheets and $RuO_2/IrO_2/TaO_2$ coated titanium rods were estimated to be 918, 1104 and 791 cm^2. The scanning electron micrograph of graphite sheet shown in Fig. 3 indicates the flaky structure of the material. The flakes have numerous grain boundaries and their orientation was observed to be very random.
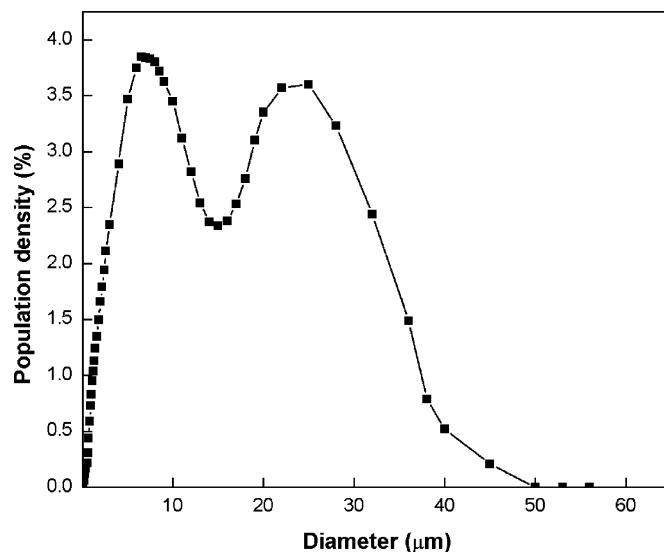

Fig. 2. Distribution of suspended solids in raw sample.

2.4. Experimental methods

For each experiment, 2 L of the effluent was transferred into the electrochemical cell and the electrodes were connected to the respective anode and cathode lead of the DC rectifier and energized for a required duration at a fixed current. During the experiment, samples were collected at different time intervals and analyzed for various parameters. After the experiment, the power was switched off and the electrodes were disconnected.

2.5. Analytical techniques

The aqueous solutions resulting from electrochemical treatment were analyzed for COD, biological oxygen demand (BOD$_5$), suspended solids, chlorides, Total Kjeldahl Nitrogen (TKN), water hardness and sulfate according to the standard

Table 1
Physico-chemical characteristics of the raw effluent and electrocoagulated sample

Parameter	Raw effluent	After electrocoagulation[a]
Color	Blackish	Pale yellow
pH	7.3	8.2
Conductivity (μmhos cm^{-1})	4490	4290
BOD$_5$ (mg L^{-1})	182	70
COD (mg L^{-1})	1316	428
Total solids (mg L^{-1})	5104	4208
Total dissolved solids (mg L^{-1})	4274	4190
Suspended solids (SS) (mg L^{-1})	830	10
Total hardness as CaCO$_3$ (mg L^{-1})	1500	590
Ca^{2+} (mg L^{-1})	240	92
Mg^{2+} (mg L^{-1})	219	87
Total alkalinity as CaCO$_3$ (mg L^{-1})	950	530
Chloride (mg L^{-1})	922	850
Sulfate (mg L^{-1})	1080	960
TKN (mg L^{-1})	70	47.3
Mean size of SS (μm)	10.14	–

[a] Electrocoagulation time: 5 min, current density: 30 mA cm^{-2} and electrode: aluminium.
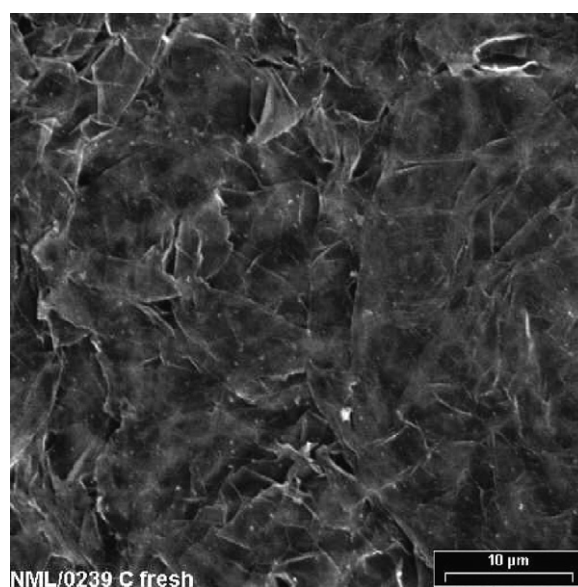

Fig. 3. Scanning electron micrograph of graphite sheet.

Table 2
Effect of current density and anode materials on COD removal by electrocoagulation

Time (min)	COD (mg L^{-1}) aluminum as anode				COD (mg L^{-1}) mild steel as anode			
	Current density (mA cm^{-2})				Current density (mA cm^{-2})			
	30	24	18	12	30	24	18	12
5	494	503	520	551	612	670	694	702
10	494	503	520	551	595	673	710	740
15	494	503	520	551	–	674	710	793
30	480	489	505	516	579	659	667	793
45	467	461	505	516	–	–	–	769
60	447	449	498	516	–	–	–	753

methods suggested by American Public Health Association [13]. COD was estimated by open reflux method. The sample was refluxed in an acidic medium with a known excess of potassium dichromate and the remaining dichromate was titrated with ferrous ammonium sulfate. The electrical conductivity and suspended solids were estimated using conductivity meter and particle size analyzer (CILAS 1180, France), respectively.

3. Results and discussion

3.1. Electrocoagulation

In the first stage, the sample was subjected to electrocoagulation to remove the suspended solids and the COD therein. Experimental results on the kinetics of COD removal at different current densities are presented in Table 2. From the results, it could be seen that the aluminum as anode was more effective compared to mild steel. The suspended solids were removed to the extent of 99% from its initial concentration of 830 mg L^{-1} within 5 min. The size distribution of the suspended solids of the effluent is shown in Fig. 2. From the distribution curve, it is apparent that the size of the suspended solids varies from 0.04 to 40 μm with a mean size of 10.14 μm. Nearly 6% (by volume) of the solids are colloidal that is below 1 μm. The Al^{3+} or Fe^{2+} ions released by anodic dissolution are expected to destabilize the suspended solids that lead to coagulation. It is known that the Al^{3+}/Fe^{2+} ions released from the anode in turn form oxyhydroxides, which are good coagulants. In addition to suspended solids, the dissolved organics that can form insoluble complexes with Fe^{2+}/Fe^{3+} ions could also be removed during electrocoagulation. The COD removal could be interpreted either due to the adsorption of dye molecules on oxy-hydroxide or due to interaction of metal ions forming insoluble metal-dye precipitate or by both mechanisms. In this case, the COD of the effluent was reduced to 500 mg L^{-1} from its initial concentration of 1316 mg L^{-1} during electrocoagulation.

The effect of current density on the removal of COD was also studied at four different current densities, i.e., 12, 18, 24 and 30 mA cm^{-2} and the results were presented in Table 2. It is evident that most of the suspended solids contributing to COD are removed within the duration of 5 min of electrocoagulation. By increasing the current density, the anodic dissolution of metal will be increased and the time required for coagulation is reduced. The amount of aluminum dissolution in 5 min at a current density of 30 mA cm^{-2} was estimated to be 70 mg L^{-1}. It may be noted that SO$_4{}^{2-}$ and Cl$^-$ ions are inevitably introduced into aqueous solutions during conventional coagulation, whereas such secondary pollution can be avoided by electrocoagulation. The total nitrogen was also decreased to 47 mg L^{-1} from its initial value of 70 mg L^{-1} during electrocoagulation. From the above discussion, it is apparent that maximum reduction of pollutants can be achieved within a short period at an applied current density of 30 mA cm^{-2}. Accordingly, required quantity of effluent was processed by electrocoagulation using aluminum electrodes and the sample was subjected to filtration. The filtrate was used for further electrooxidation studies.

3.2. Electrooxidation

3.2.1. Effect of electrode material

Two different materials, viz. RuO$_2$/IrO$_2$/TaO$_2$ coated titanium and graphite were used as electrodes during electrooxidation. The decrease in COD and Cl$^-$ with time at a constant current density was monitored and the results are shown in Fig. 4a and b. The decrease in COD was observed to be hardly 80 mg L^{-1} in the presence of RuO$_2$/IrO$_2$/TaO$_2$ coated titanium electrodes whereas more than 380 mg L^{-1} decrease could be observed using graphite sheets. Though the decrease in COD was very marginal in the presence of RuO$_2$/IrO$_2$/TaO$_2$ coated titanium, the complete decoloration of the effluent was achieved within 5 min. The rate of COD removal during the initial stages of the electrooxidation was observed to be high especially with graphite electrodes. The decrease in rate of COD removal at latter stages may be attributed to the formation of stable intermediates. From the chloride ion measurements shown in Fig. 4b, it is evident that the decrease in chloride ion concentration is hardly 70 mg L^{-1} in the presence of RuO$_2$/IrO$_2$/TaO$_2$ coated titanium electrodes and above 400 mg L^{-1} in the presence of graphite sheet. In general, it is evident that as the concentration of Cl$^-$ ion decreases, the COD also proportionately decreased. This implies that the oxidation of organics depends mostly on active chlorine generated during electrolysis. Serikawa et al. [14] have observed strong catalytic effect in the conversion of organic pollutants to innocuous CO$_2$ and H$_2$O in the presence of chloride ion. It also indicates that the indirect electrooxidation involving various forms of chlorine was a predominant process in removing organic pollutants from chloride medium. The electrochemical
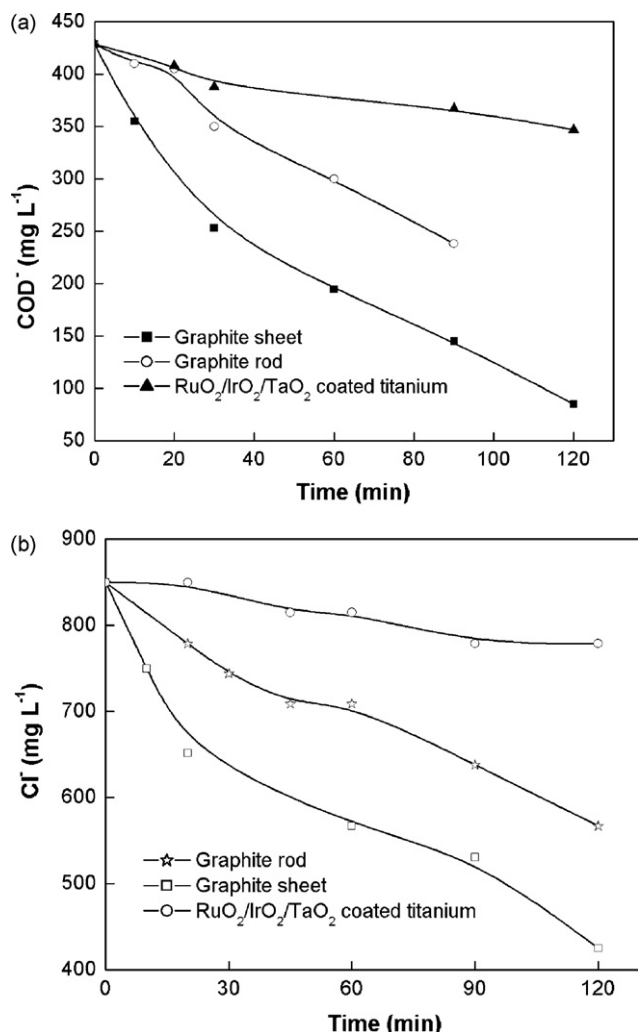
Fig. 4. (a) Influence of electrode materials on COD reduction at a constant current of 5 A. (b) Influence of electrode materials on chloride reduction at a constant current of 5 A.

discharge of chlorine at the anode as secondary electrochemical reaction can be represented as

$$2Cl^- \rightarrow Cl_{2(g)} + 2e^- \tag{1}$$

At 25 °C and normal atmospheric pressure, the chlorine gas thus liberated from anode can dissolve in water to the extent of 6.413 g L^{-1} [15]. If its solubility is exceeded locally at the electrode surface, then bubbles may form. Above pH 3.3, the chlorine will be diffused to the bulk aqueous solution away from the electrode and establishes equilibrium between chlorine, hypochlorous acid and hypochlorite ion. Since the experiments were conducted around neutral pH, only HOCl and OCl$^-$ species are expected in aqueous solution. An attempt was made to estimate the concentration of free chlorine in aqueous solution by iodometric method (No. 4500–Cl B) suggested by APHA [13]. The concentration of free chlorine was found to be more than the Cl$^-$ that got depleted from the aqueous system. This could be presumed due to other oxidizing agents generated during electrolysis. It may be noted that H$_2$O$_2$ will interfere in the quantitative estimation of free chlorine.

It is known that the oxygen evolution is a primary reaction at the anode surface in dilute chloride solutions. The anodic oxygen evolution could be represented as

$$2H_2O \rightarrow O_2 + 4H^+ + 4e^- \tag{2}$$

The cathodic conversion of molecular oxygen to active oxygen in the presence of chloride ion [14] can be represented as

$$4H_2O + 2O_{2(aq)} + 4e^- \rightarrow 2H_2O_2 + 4OH^- \tag{3}$$
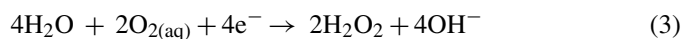
Production of ozone also is expected when the anode potential exceeds beyond 1.51 V and also by oxidation of evolved oxygen [16].

$$H_2O + O_2 \rightarrow O_3 + 2H^+ + 2e^- \tag{4}$$
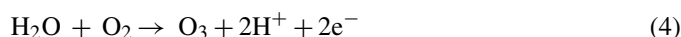
Szpyrkowicz et al. [17] have suggested the generation of various oxidants such as nascent oxygen, ozone, hydrogen peroxide, free chlorine and free radicals such as ClO$^\bullet$, Cl$^\bullet$, and OH$^\bullet$ during electrolysis. Thus, the aqueous solution may contain a cocktail of oxidants. In the absence of procedures for the estimation of various oxidants, it is very difficult to obtain the quantitative picture of the various oxidants in aqueous solution. Since the solubility of oxygen and ozone in water is very less, it is presumed that HOCl and H$_2$O$_2$ are the main oxidants that are responsible for degradation of organics. Low degradation of organics in the presence of RuO$_2$/IrO$_2$/TaO$_2$ coated titanium could be explained due to the competition between the oxidation of organics and the oxygen evolution reaction at the anode surface. Though the current efficiency is comparatively poor, selective degradation can be achieved by using these electrodes. The selective oxidation of organics on noble oxide catalytic anode was attributed to the formation of "higher oxides" [18] via adsorption of hydroxyl radical and its interaction with the oxygen already present in the oxide with the possible transition to higher oxide.

$$MO_x + {}^\bullet OH \rightarrow MO_x({}^\bullet OH) \rightarrow MO_{x+1} + H^+ + e^- \tag{5}$$
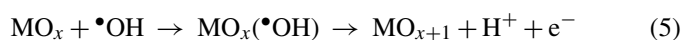
Better removal of organics in the presence of graphite electrode could be attributed to the generation of HOCl and H$_2$O$_2$ which are stronger oxidants compared to oxygen. Also, due to their high solubility, the build up concentration will become so high that the refractory organics could be easily oxidized. Raghu and Basha [19] have suggested that the oxidation of organics in the presence of chloride ion proceeds via adsorption of $^\bullet$OCl on metal oxide and possible transition of oxygen atom to metal oxide forming higher metal oxide on the similar lines mentioned in Eq. (5).

Regarding total nitrogen, it was eliminated below the detectable limit in the presence of graphite sheet and only 40% in the presence of RuO$_2$/IrO$_2$/TaO$_2$ coated titanium. The electrochemical reduction of nitrate ions can be represented as

$$NO_3{}^- + 3H_2O + 5e^- \rightarrow 0.5N_2 + 6OH^- \tag{6}$$

$$NO_3{}^- + 6H_2O + 8e^- \rightarrow NH_3 + 9OH^- \tag{7}$$
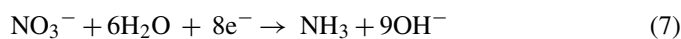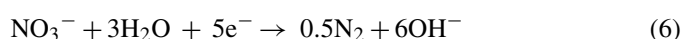
The direct and indirect electrochemical oxidation of ammonia in the presence of OH$^-$ and Cl$^-$ can be represented as

$$2NH_3 + 6OH^- \rightarrow N_2 + 6H_2O + 6e^- \tag{8}$$
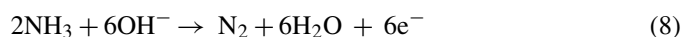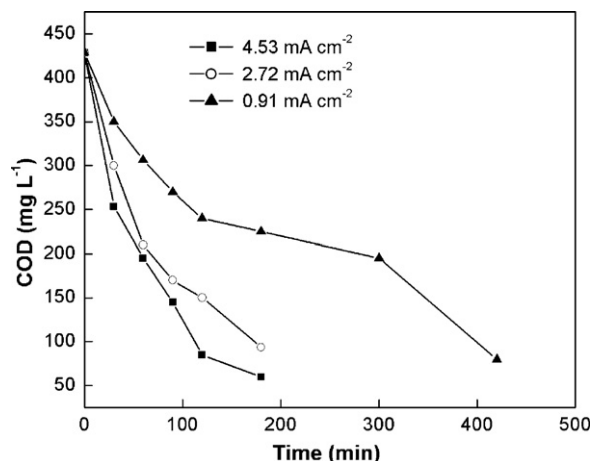
Fig. 5. Effect of current density on COD reduction in the presence of graphite sheet.

$$2NH_3 + 6Cl^- \rightarrow N_2 + 6HCl + 6e^- \qquad (9)$$
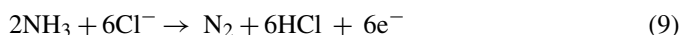
From the present study it is evident that the degradation of organics in the presence of graphite is better compared to $RuO_2/IrO_2/TaO_2$ coated titanium. Among the graphite materials used, the performance of rods is slightly inferior compared to sheet. This may be presumed due to the surface morphology and geometry of the electrodes which needs further study.

3.2.2. Effect of current density

The effect of current density on the electrochemical oxidation of organics in the presence of different electrodes was studied and the results are shown in Figs. 5–7. From the results it is evident that as the current density is increased the rate of oxidation is increased. In the case of $RuO_2/IrO_2/TaO_2$ coated titanium, the effect of current density is very marginal. Though the current density was increased from 3.79 to 6.32 mA cm^{-2}, the COD remained at 347 mg L^{-1}. Similarly, the rate of COD removal in the presence of graphite rods is marginal at 1.08 mA cm^{-2}. However, it was gradually increased as the current density was
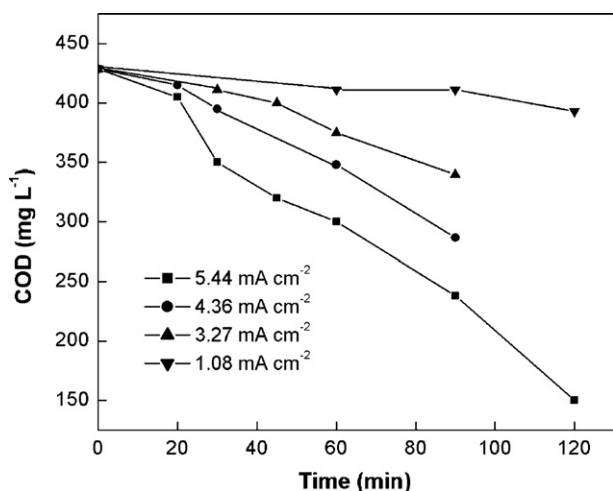

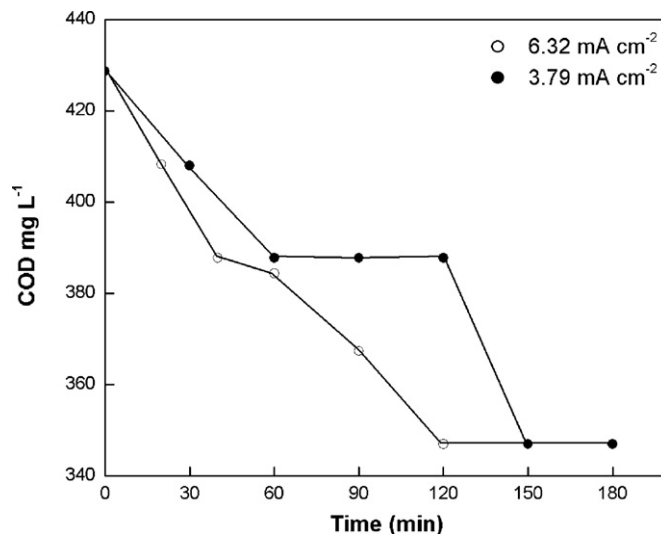Fig. 6. Effect of current density on COD reduction in the presence of graphite rod.

Fig. 7. Effect of current density on COD reduction in the presence of $RuO_2/IrO_2/TaO_2$ coated titanium.

increased from 3.27 to 5.44 mA cm^{-2}. Under a given set of experimental conditions, the rate of generation of active chlorine remains constant, but expected to vary with the applied current density. Then

$$\frac{I_A}{zF} = k_{obs}[\text{Eff}] = k[\text{COD}] \qquad (10)$$

The electrochemical reaction rate (for removal of COD) for the batch reactor is

$$-\left[\frac{V_R}{A_e}\right]\frac{d[\text{COD}]}{dt} = \frac{I_A}{zF} = k_m[\text{COD}] \qquad (11)$$

On integrating the above Eq. (11)

$$\ln\frac{\text{COD}_0}{\text{COD}} = k_m at \qquad (12)$$

$a = A_e/V_R$ where a is the specific area of electrode in cm^{-1}, V_R is volume of the reactor in cm^3, A_e is surface area of the electrode in cm^2, I_A is applied current in A, F is Faraday's Constant (96,487 C mol^{-1}), d[COD]/dt is decrease in COD with respect to time (g cm^{-3} s^{-1}) and k_m is mass transfer co-efficient (cm s^{-1}).

The instantaneous current efficiency (ICE) was calculated using

$$\text{ICE} = \frac{[(\text{COD})_t - (\text{COD})_{t+\Delta t}]}{8I_A\Delta t}FV \qquad (13)$$

COD$_t$ and COD$_{t+\Delta t}$ are the chemical oxygen demand at time t and $t + \Delta t$, respectively, in (g L^{-1}), V is the volume of effluent in litres, I_A is applied current in A, Δt is change in time in seconds.

The energy consumption (E) was calculated using

$$E = \frac{I_A V_A t}{V \times \Delta\text{COD} \times 3600} \qquad (14)$$

V_A is the applied voltage in volts, ΔCOD decrease in COD values in g L^{-1}, t is the electrooxidation time in seconds. The current consumption, ICE and mass transfer coefficient were

Table 3
The instantaneous current efficiency (ICE), mass transfer coefficient (k_m) and energy consumption (E) values for different anode materials

Anode materials											
Graphite sheet				Graphite rod				Titanium rod			
C.D.[a]	ICE (%)	k_m (10^{-4} cm s^{-1})	E (kWh g^{-1})	C.D.[a]	ICE (%)	k_m (10^{-4} cm s^{-1})	E (kWh g^{-1})	C.D.[a]	ICE (%)	k_m (10^{-4} cm s^{-1})	E (kWh g^{-1})
4.528	19.1	6.07	0.07	5.446	20.1	3.38	0.10	6.32	5.42	1.46	0.24
2.717	27.4	4.64	0.03	3.267	23.9	1.05	0.07	3.792	10.6	0.82	0.20
0.905	44.4	2.10	0.02	1.089	44.2	0.341	0.05				

[a] Current density in mA cm^{-2}.

calculated at different current densities for $RuO_2/IrO_2/TaO_2$ coated titanium, graphite sheet and graphite rods and the results are compiled in Table 3. Depending on the current density, the ICE values were observed to vary from 20 to 45%. Accordingly, the energy consumption was also reduced from 0.24 to 0.02 kWh g^{-1}. It is apparent that electrooxidation at lower current densities is advantageous. It was reported that CE of 70% was observed at low current densities of 0.03–0.32 A m^{-2} for graphite electrodes [20]. When the current density was increased to 10–100 A m^{-2}, the current efficiency values decreased to 6–17% [20]. The low ICE values of 5–10% and high energy consumption (0.24 kWh g^{-1}) observed in the case of $RuO_2/IrO_2/TaO_2$ coated titanium electrodes may be interpreted due to the formation of stable intermediate compounds. Among the various electrodes used, graphite sheet has exhibited high mass transfer coefficient value of 6.07×10^{-4} cm s^{-1}. The k_m value was observed to increase as the current density is increased. With regard to ICE, k_m and energy consumption values, the behavior of graphite materials was observed to be different from that of $RuO_2/IrO_2/TaO_2$ coated titanium.

4. Conclusions

Wastewater from the textile industry was processed by electrocoagulation and electrooxidation techniques. The suspended solids were removed to the extent of 99% from its initial concentration of 830 mg L^{-1} by electrocoagulation within 5 min. The initial COD of 1316 mg L^{-1} was reduced to 494 mg L^{-1} in the presence of Al electrodes. After electrocoagulation, the effluent was further subjected to electrooxidation using two different materials, viz. graphite and $RuO_2/IrO_2/TaO_2$ coated titanium as anodes. The decrease in COD is hardly 80 mg L^{-1} in the presence of $RuO_2/IrO_2/TaO_2$ coated titanium electrodes whereas more than 380 mg L^{-1} was decreased in the presence of other electrodes. Graphite was observed to be more efficient for anodic incineration of organics compared to $RuO_2/IrO_2/TaO_2$ coated titanium. The Cl$^-$ ion depletion during electrooxidation indicated the generation of free chlorine. As the Cl$^-$ ion depletion increases, the COD removal was also increased. Graphite electrode has exhibited higher ICE values of 45%, whereas $RuO_2/IrO_2/TaO_2$ coated titanium yielded only 10%. The ICE was increased to 2 folds by decreasing the current density from 4.53 to 0.91 mA cm^{-2}. Similarly, the energy consumption was reduced to 0.02 kWh g^{-1} from 0.07 kWh g^{-1} by decreasing the current density. With regard to ICE, k_m and energy consumption values, the behavior of graphite material was observed to be different from that of $RuO_2/IrO_2/TaO_2$ coated titanium.

References

[1] I. Arslan-Alaton, Color. Technol. 119 (2003) 345–353.

[2] H. Kusic, N. Koprivanac, A.L. Bozic, Chem. Eng. J. 123 (2006) 127–137.

[3] C. Wang, A. Yediler, D. Lienert, Z. Wang, Chemosphere 52 (2003) 1225–1232.

[4] N. Daneshvar, H. Ashassi-Sorkhabi, A. Tizpar, Sep. Purif. Technol. 31 (2003) 153–162.

[5] M. Kobya, O.T. Can, M. Bayramoglu, J. Hazard. Mater. 100 (2003) 163–178.

[6] M. Muthukumar, M.T. Karuppiah, G.B. Raju, Sep. Purif. Technol. 55 (2007) 198–205.

[7] J. Jia, J. Yang, J. Liao, W. Wang, Z. Wang, Water Res. 33 (1999) 881–884.

[8] Z. Shen, W. Wang, J. Jia, J. Ye, X. Feng, A. Peng, J. Hazard. Mater. 84 (2001) 107–116.

[9] A. Fernandes, A. Morao, M. Magrinho, A. Lopes, I. Goncalves, Dyes Pigments 61 (2004) 287–296.

[10] S. Hattori, M. Doi, E. Takahashi, T. Kurosu, M. Nara, S. Nakamatsu, Y. Nishiki, T. Furuta, M. Iida, J. Appl. Electrochem. 33 (2003) 85–91.

[11] J. Naumczyk, L. Szpyrkowicz, F. Zilio-Grandi, Water Sci. Technol. 34 (1996) 17–24.

[12] A.G. Vlyssides, M. Loizidou, P.K. Karlis, A.A. Zorpas, D. Papaioannou, J. Hazard. Mater. 70 (1999) 41–52.

[13] APHA, AWWA, WPCF, Standard Methods for the Examination of Water and Wastewater, 20th ed., American Public Health Association, Washington, DC, 1998.

[14] R.M. Serikawa, M. Isaka, Q. Su, T. Usui, T. Nishimura, H. Sato, S. Hamada, J. Appl. Electrochem. 30 (2000) 875–883.

[15] Norbert Adolph Lange (Ed.), Handbook of Chemistry, 10th ed., McGraw Hill book Company, London, 1967.

[16] D. Pletcher, F.C. Walsh, Industrial Electrochemistry, Blackie Academic & Professional, Glasgow, 1993.

[17] L. Szpyrkowicz, S.N. Kaul, R.N. Neti, S. Satyanarayan, Water Res. 39 (2005) 1601–1613.

[18] M. Panizza, G. Cerisola, Environ. Sci. Technol. 38 (2004) 5470–5475.

[19] S. Raghu, C.A. Basha, J. Hazard. Mater. 139 (2007) 381–390.

[20] G. Chen, Sep. Purif. Technol. 38 (2004) 11–41.